

# Combination of Silver Nanoparticles and Vancomycin to Overcome Antibiotic Resistance in Planktonic/Biofilm Cell from Clinical and Animal Source

Mahmoud S.M. Mohamed,<sup>1,\*</sup> Heba M. Mostafa,<sup>1,\*</sup> Sara H. Mohamed,<sup>2</sup>  
Sherein I. Abd El-Moez,<sup>3</sup> and Zeinat Kamel<sup>1</sup>

This study aims to evaluate the prevalence of multidrug-resistant (MDR) and biofilm-forming pathogens from animal source compared to clinical ones. In addition, to assess the antibacterial and antibiofilm activity of silver nanoparticles (AgNPs) alone and/or mixed with vancomycin. Out of 62 bacterial isolates from animal respiratory tract infection (RTI), 50.00% were defined as MDR, while among human ones, 44.00% were MDR. The bacteria *Staphylococcus aureus*, *Pseudomonas aeruginosa*, and *Streptococcus pneumoniae* were the predominant isolated bacteria from both animal and human origin with frequency percentage of 50.00, 22.32, and 18.75, respectively. Among *Staph. aureus* strains, *mecA* gene was detected in 60.00% and 61.54% of animal and human isolates, respectively, while *mec<sub>ALGA251</sub>* (*mecC*) gene was detected in 13.33% and 15.38% of animal and human isolates, respectively. Biofilm formation ability among animal isolates was 83.87%, while among human ones was 86.00%. AgNPs were effective in inhibiting planktonic cells with minimal inhibitory concentration (MIC) values (0.625–10 µg/mL), as well as eradicating biofilm with minimal biofilm eradication concentration values (1.25–10 µg/mL). Noticeable low MIC of AgNPs was required for the isolates from animal source (0.625–5 µg/mL) compared to clinical ones (0.625–10 µg/mL). Remarkable reduction in AgNP effective concentration was observed after combination with 1/4 MIC of vancomycin with minimum recorded concentration of 0.08 µg/mL. In conclusion, the prevalence of MDR among RT pathogens was recorded with high ability to produce biofilm and virulence factors from both animal and human pathogens. AgNPs showed strong antibacterial and antibiofilm activity alone and mixed with vancomycin, with up to fourfold reduction of AgNP inhibitory dose.

**Keywords:** silver nanoparticles (AgNPs), vancomycin, biofilm, respiratory tract infection (RTI)

## Introduction

**P**ATHOGENIC BACTERIA REMAIN a major health concern responsible for causing a large number of hospitalizations and deaths each year, and due to the extensive usage of antibiotics, bacteria are exponentially gaining resistance to those antibiotics at an alarming rate.<sup>1,2</sup> The scarcity of new drug development by the pharmaceutical industry, due to reduced economic incentives and challenging regulatory requirements, complicates the treatment of infectious diseases.<sup>3</sup> Indeed, exposure of pathogens to antimicrobial agents such as antibiotics gives high opportunities for bacterial pathogens to become less susceptible toward antibiotics, by altering the cell structure as well as cellular metabolism.<sup>4</sup>

Respiratory tract infections (RTIs) are one of the most common causes of illness from infectious pathogens worldwide and the leading cause of increased mortality in geriatrics, children, and immunocompromised persons, due to the lack of medication.<sup>5</sup> RTIs are known as any infectious disease of the upper (URTIs) or lower (LRTIs) respiratory tract. URTIs involve the common cold, tonsillitis, rhinitis, and others, while LRTIs include acute bronchitis and pneumonia.<sup>6</sup> The traditional way to prevent and treat infections such as RTIs is the use of commercial antibiotics, but currently, the outbreak of resistant bacteria makes antibiotics invaluable weapons to fight against pathogens, which brings a great concern to the health of both humans and animals.<sup>7</sup>

The URT would appear to be an ideal target for bacterial colonization and biofilm growth because it is moist, warm,

<sup>1</sup>Department of Botany and Microbiology, Faculty of Science, Cairo University, Giza, Egypt.

<sup>2</sup>Department of Microbiology, National Organization for Drug Control and Research, Giza, Egypt.

<sup>3</sup>Department of Microbiology and Immunology, Veterinary Research Division, National Research Center, Dokki, Giza, Egypt.

\*These authors contributed equally to this article.

and easily accessible to airborne pathogens. It was reported that many of URT pathogens are known to form biofilms efficiently.<sup>8</sup> Many studies demonstrated that, the high resistance rate recorded in those biofilms seems to not be genotypic; instead, it is rather due to multicellular strategies and/or to the ability of individual cells, contained inside the biofilm, to differentiate in a protected phenotypic state.<sup>9,10</sup>

Over the past few years, synthesis and characterization of nanoparticles have gained increasing momentum and has immense potential to revolutionize in the biomedical research by developing new and improved products for clinical diagnosis and therapy.<sup>11</sup> Silver has become one of the most universal antimicrobial substances, especially after expanding the surface area of silver particles by nanoengineering.<sup>12,13</sup>

Nowadays, great attention was given toward biomedicine-related assessment of silver nanoparticles (AgNPs), as unconventional antimicrobial agents. Even though there is no enough information about their toxicity as well as their *in vivo* biological behavior, these structures were used as antimicrobial agents in different fields such as health care, cosmetic products, medicinal devices sterilization, and others for a long time.<sup>14</sup> The main problem remaining in the use of AgNPs is the toxicity concerns; therefore, effective antimicrobial dose of AgNPs with low concentration against the multidrug-resistant (MDR) pathogens is a crucial goal of many researchers.

This study aimed to evaluate the prevalence of antibiotic resistance, virulence factors and biofilm formation ability of RTI pathogens from human pathogens compared with animal ones. In addition, to study the antibacterial and antibiofilm activity of AgNPs alone and/or mixed with antibiotics against RTI pathogens to reduce the effective antimicrobial dose and consequently, reduce the possible AgNP negative *in vivo* biological behavior in host.

## Materials and Methods

### Bacterial collection and identification

This study was performed on 112 unduplicated bacterial isolates collected from two different places: Kasr El-Ainy hospital (50 isolates) during the period of March 2014 to June 2014, and National Center for Research on Animal Health (62 isolates) from November 2013 to March 2014. Identification was done using microscopic examination and biochemical identification according to Bergey manual.<sup>15</sup> Isolates were identified biochemically based on colony morphology on MacConkey's agar and blood agar, Gram staining, and laboratory biochemical tests, including catalase, coagulase, urease, citrate, oxidase, motility indole ornithine, methyl red, triple sugar iron, Voges Proskauer, and lactose fermentation ability. Subsequently, selective media such as mannitol salt agar and cefrimide agar were used for *Staphylococcus aureus* and *Pseudomonas aeruginosa* cultivation, respectively.

### Antibiotic susceptibility test

The susceptibility of all bacterial isolates was determined on Müller Hinton agar (MH; Laboratories Conda SA, Madrid, Spain) by disc diffusion method according to Clinical and Laboratory Standards Institute (CLSI) recommendations<sup>16</sup> using available antibiotic discs (Oxoid, Basingstoke, UK) of gentamicin (10 µg), vancomycin (30 µg), ampicillin (10 µg), ciprofloxacin (5 µg), erythromycin (15 µg), amoxicillin (30 µg), clindamycin (2 µg), and ceftiofloxacin (30 µg). After incubation at 37°C for 24 h, zones of inhibition were measured, and isolates were classified as susceptible (S), intermediate (I), or resistant (R) according to the criteria of the CLSI guidelines.<sup>17</sup>

### Detection of *mecA* and *mecC* genes by polymerase chain reaction

**DNA extraction and primers used.** Genomic DNA was extracted by using Gene JET Genomic DNA purification kit (Thermo Scientific), in which lysostaphin (Sigma-Aldrich, St. Louis, MO) was added to an overnight grown bacterial culture at final concentration of 100 µg/mL and then incubated at 37°C for 1 h. The presence of *mecA* and *mecC* (*mecALGA251*) was detected by polymerase chain reaction (PCR) as described before using primers listed in Table 1.<sup>18</sup>

**Reaction conditions.** PCR was performed in a total volume of 25 µL, containing 3 µL genomic DNA template (~50 ng), 1 µL of each primer, and 12.5 µL OnePCR™ Plus master mix (GeneDirex), and finally, water was added to make volume up to 25 µL. PCR amplification was done with thermal cycler (Applied Biosystems 9700; PE Life Sciences, New York) programmed with initial denaturation for 5 min at 94°C, and then 30 cycles: denaturation for 30 sec at 94°C, annealing for 30 sec at 55.5°C, extension at 72°C for 30 sec, and a final extension at 72°C for 7 min. After amplification, 10 µL of each PCR product was analyzed on 1.5% agarose gel stained with ethidium bromide (0.5 µg/mL) and then visualized under ultraviolet light. The Gene Ruler 100 pb DNA ladder (GeneDirex) was used as a DNA size marker.<sup>18</sup>

### Detection of virulence factors

**Enzymatic activity.** Phenotypic detection of blood hemolysis and gelatinase, and DNase tests were done according to the recommended method.<sup>19</sup> Brain heart infusion (BHI) agar (Oxoid) supplemented with 5% (v/v) horse blood was used to test blood hemolysis, at which the formation of clear colorless ( $\alpha$ -hemolysis) or clear greenish ( $\beta$ -hemolysis) zones around the bacterial growth was considered a positive result. For gelatinase activity, the positive result was determined by liquefaction of gelatin medium after refrigerator incubation for 4 h. DNase activity was tested using DNase agar medium plates inoculated with the test organism,

TABLE 1. PRIMERS USED IN THIS STUDY

Primer	Sequence	Amplicon size (bp)
<i>mecA</i> P4	5'-TCCAGATTACAACCTTACCAGG-3'	162
<i>mecA</i> p7	5'-CCACTTCATATCTTGTAACG-3'	
<i>mecA</i> <sub>LGA251</sub>	5'-GAAAAAAAGGCTTAGAACGCCTC-3'	138
<i>mecA</i> <sub>LGA251</sub>	5'-GAAGATCTTTCCGTTTTTCAGC-3'	

incubated at 37°C for 18–24 h, and then the plates were flooded with 1 N hydrochloric acid. Observation of a clear zone around the streak was considered a positive result.

**Biofilm formation.** The presence and activity of biofilm formation were assessed with colorimetric methods based on crystal violet dye. Briefly, a 0.5 MacFarland bacterial culture in BHI broth was used to inoculate wells in a 96-well microtiter polystyrene plate. After incubation for 18 h at 37°C, the plates were gently washed thrice with phosphate-buffered saline (PBS) pH 7.4. The adherent bacterial films were left to air dry and then stained with 1% crystal violet aqueous solution for 20 min, then excess stain was rinsed off with tap water. Optical densities (OD) were measured at 570 nm by an automatic microplate reader (Stat Fax-2100; GMI, Inc.).

The ability to form biofilm was scored and categorized as follows: (OD ≤ OD<sub>c</sub>), (2 OD<sub>c</sub> < OD ≤ 4 OD<sub>c</sub>), and (4 OD<sub>c</sub> < OD) as non-biofilm, moderate biofilm, and strong biofilm forming, respectively, where OD<sub>c</sub> is the cutoff value, which is defined as three standard deviations above the negative control mean OD.<sup>20</sup>

#### Preparation and characterization of AgNPs

AgNPs prepared by chemical reduction of silver nitrate (AgNO<sub>3</sub>) with glucose in the presence of protective agent polyvinylpyrrolidone (Sigma-Aldrich) were used. Sodium hydroxide was used to enhance the reaction velocity.<sup>21</sup> The UV-Vis absorption spectra were obtained using spectrophotometer USB2000+VIS-NIR (Ocean Optics, Inc., Dunedin, FL). By using high-resolution transmission electron microscopy (TEM) JEM-2100 (JEOL Korea Ltd., Korea), size and shape of AgNPs were characterized at an accelerating voltage of 20 kV.

#### Antibacterial effect of AgNPs against bacterial isolates

**Minimum inhibitory concentrations.** Antibacterial activity of AgNPs was carried out by microtiter broth dilution method according to CLSI document M07-A9.<sup>16</sup> As a diluent, MH broth was used where about 10<sup>5</sup> CFU/mL cells (0.5 MacFarland bacterial cultures) were inoculated, at which the final volume in each microtiter plate well was 100 μL. The microtiter plates were sealed with parafilm and incubated for 24 h at 37°C to determine the minimum inhibitory concentration (MIC) values. The MIC is defined as the lowest concentration of AgNPs, which inhibited 90% of the growth when compared with that of growth control in μg/mL.

**Minimum bactericidal concentration.** After MIC determination of the AgNPs, an aliquot of 10 μL from all wells in which no visible bacterial growth was observed was seeded in MH agar plates. The plates were then incubated overnight at 37°C for 24 h. The minimum bactericidal concentration (MBC) is defined as the lowest concentration of antimicrobial agent that kills >99.9% of the initial bacterial population where no visible growth of the bacteria was observed.<sup>16</sup>

**Minimal biofilm eradication concentration.** The biofilm degrading activity of AgNPs was determined and measured on overnight grown biofilm. Briefly, all the tested bacteria were grown overnight in BHI broth, and then 100 μL of bacterial culture (0.5 MacFarland) was dispensed into each well of

microtiter plate. After 24 h of incubation at 37°C, the wells of microtiter plate were gently washed thrice with PBS pH 7.4 to remove the planktonic cells, and then filled with 100 μL twofold dilutions of the AgNPs in MH broth, ranging from MIC to 10×MIC. The plates were incubated for 24 h at 37°C, then the medium was discarded, and each well was washed twice with PBS, dried, then stained for 20 min with crystal violet solution (1% w/v), and finally washed with sterile water. The stained biofilms were resuspended using 200 μL absolute ethanol. The absorption was measured at 570 nm using a microplate reader. The negative control was MH broth only, while the positive control contained biofilm cells alone without treatment.<sup>22</sup> The experiment was performed in triplicates.

#### Preliminary screening for synergistic effect of AgNPs and vancomycin by disc diffusion method

To determine the synergistic or antagonistic effect between AgNPs and vancomycin, suspension of vancomycin-resistant *Staph. aureus* (0.5 MacFarland) was spread over MH agar medium. After 10 min, a sterile filter paper loaded with AgNPs, at the MIC concentration of the tested bacteria, was put onto the medium and different concentrations of AgNPs were added to a standard vancomycin disc (30 μg). The plates were incubated for 24 h at 37°C. Vancomycin disc (30 μg) without any AgNP was considered a negative control.<sup>23</sup>

#### Combination of AgNPs and vancomycin by microbroth dilution method

Synergy between AgNPs and vancomycin has been further confirmed by using microdilution assay,<sup>24</sup> by determining the MIC of AgNPs in presence of vancomycin at a low concentration (1/4 MIC). Fifty microliters of vancomycin at 1/4 MIC was added to a well of 96-well polystyrene microplate containing 50 μL of AgNP dilution and then inoculated with 100 μL (0.5 MacFarland) bacterial culture. MIC was defined as the lowest concentration of AgNPs, in combination with vancomycin at 1/4 MIC, inhibiting the visible growth of tested strains.

#### Statistical analysis

Pearson's chi-square test was performed to evaluate antibiotic resistance patterns of bacteria among the two groups (animal and human), at which *p* values below 0.05 were considered significant.

## Results

In this study, 112 isolates were recovered from different clinical RTI samples. Identification of bacterial isolates by biochemical tests is presented in Table 2. By comparing bacterial resistance pattern from animal and human origin, noticeable resistance to gentamicin among human isolates was detected (*p* < 0.05) (Fig. 1). The highest resistance of animal isolates was exhibited against ampicillin (72%) and erythromycin (74%) (Fig. 1A), while for human ones (Fig. 1B), the highest resistance was exhibited against gentamicin (82.26%) and amoxicillin (74.19%). Susceptibility to vancomycin was 41.94% and 40% among animal and human strains, respectively.

The isolated bacteria were characterized as MDR according to the definition of MDR as the nonsusceptibility of

TABLE 2. PERCENTAGE AND SOURCE OF RESPIRATORY TRACT INFECTION BACTERIAL ISOLATES COLLECTED FROM ANIMAL AND HUMAN SAMPLES

Bacterial species	Isolate source			
	Animal		Human	
	Percentage	n	Percentage	n
Gram positive	69	43	76	38
<i>Staphylococcus aureus</i>	48	30	52	26
<i>Streptococcus pneumoniae</i>	15	9	24	12
<i>Listeria monocytogenes</i>	6	4	—	—
Gram negative	31	19	24	12
<i>Pseudomonas aeruginosa</i>	21	13	24	12
<i>Klebsiella pneumoniae</i>	10	6	—	—
Total	100	62	100	50

bacteria to at least one agent in three or more antimicrobial categories.<sup>25</sup> Out of 62 bacterial isolates recovered from diseased animals, 31 (50%) were defined as MDR, while among human ones, 22 (44%) MDR isolates were found. About 15 (50%) and 10 (38.46%) *Staph. aureus* strains among animal and human, respectively, were defined as MDR.

On the other hand, *mecA* and *mecC* genes were assayed, and the results showed that *mecA* gene was detected in 60% and 61.54% of animal and human isolates, respectively, while

*mecC* gene was detected in 13.33% and 15.38% of animal and human isolates, respectively. On the other hand, 26.67% and 23.08% from animal and human isolates, respectively, were negative for both genes.

Different virulence factors were screened and as a result, all *Staph. aureus* and *Ps. aeruginosa* isolates from animal and human sources were found to be positive for gelatinase production (Table 3). Among animal isolates, all *Staph. aureus* (100%) isolates and *L. monocytogenes* (100%) were positive for DNase. All *Strep. pneumoniae* and *L. monocytogenes* were positive for haemolysin, whereas 67% of *Staph. aureus* isolates and 53.85% of *Ps. aeruginosa* were positive for haemolysin. On the other hand, among human isolates, DNase was detected only in *Staph. aureus* (100%). *Ps. aeruginosa* and *Strep. pneumoniae* were positive for hemolysin (100%), whereas 69% of *Staph. aureus* was positive for hemolysin.

Biofilm formation ability was assayed by using tissue culture plate method. Biofilm formation ability was seen in 52 (83.87%) animal bacterial isolates, in which 39 isolates were Gram positive and 13 were Gram negative, while among human isolates, 43 out of 50 bacterial tested isolates had the ability to form biofilm (86%). Biofilm formers were characterized in 50% and 52% among animal and human bacterial isolates, respectively (Table 4).

Water-soluble AgNPs had a yellow color in solution at 1,000 ppm concentration (optical prop. [Abs.]  $\lambda_{max}$ =410 nm, Avg.). The absorption spectra of AgNPs are represented in Fig. 2, indicating that this sample depicted a well-defined single plasmon band at ~401 nm, which is characteristic for

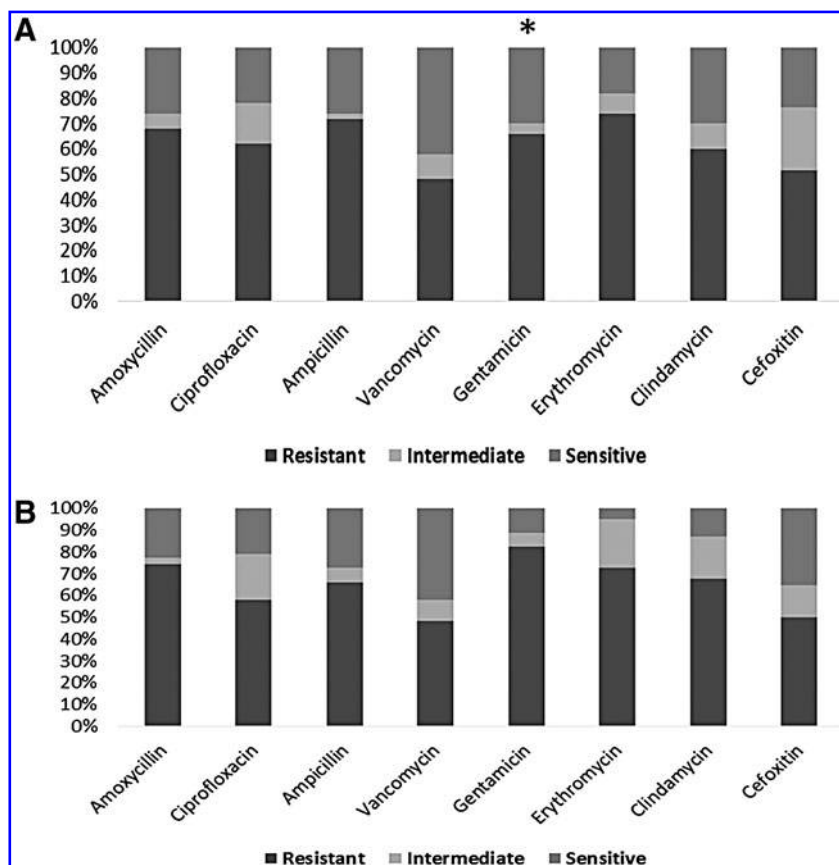


FIG. 1. Resistance, intermediate, and sensitivity rates of antibiotics against bacterial isolates from animal (A) and human (B). \*Result is significant at  $p < 0.05$  according to the chi-square statistic.

TABLE 3. COMPARISON OF VIRULENCE FACTOR PERCENTAGES AMONG ANIMAL ( $n=62$ ) AND HUMAN ( $n=50$ ) ISOLATES

Isolates	Percentage of virulence factor					
	Gelatinase		Dnase		Hemolysin	
	Animal	Human	Animal	Human	Animal	Human
Gram positive						
<i>Staphylococcus aureus</i>	100	100	100	100	66.66	69.23
<i>Streptococcus pneumoniae</i>	—	—	—	—	100	100
<i>Listeria monocytogenes</i>	—	—	100	—	100	—
Gram negative						
<i>Pseudomonas aeruginosa</i>	100	100	—	—	53.85	100
<i>Klebsiella pneumoniae</i>	—	—	—	—	—	—

nanosized silver. The TEM micrographs presented in Fig. 3A showed the spherical shape of AgNPs, in which the particle size ranged between 5 and 21 nm and an average size of  $11.07 \pm 2.8$  (Fig. 3B).

By comparing MIC and MBC of AgNPs (Table 5), AgNPs were effective in inhibiting planktonic cells at low concentration, ranging from 0.625–5  $\mu\text{g/mL}$  to 0.625–10  $\mu\text{g/mL}$  for animal and human isolates, respectively. In most cases, MBC for tested bacteria was higher than MIC, values ranging from 1.25–5  $\mu\text{g/mL}$  to 1.25–20  $\mu\text{g/mL}$  for animal and human isolates, respectively. The eradication activity of AgNPs against biofilm-embedded bacteria as analyzed by minimal biofilm eradication concentration (MBEC) revealed that the values of most isolates were higher than MIC values of planktonic cells, they ranged from 1.25–5  $\mu\text{g/mL}$  to 1.25–10  $\mu\text{g/mL}$  for animal and human, respectively. It was observed that the biofilm of *Staph. aureus* human strains was less affected by AgNPs compared to other bacterial isolates.

Preliminary screening for synergistic effect of AgNPs and vancomycin was done to vancomycin-resistant *Staph. aureus* grown, showing noticeable inhibition zones/synergistic effect by adding AgNPs with different concentration to blank vancomycin antibiotic disk (Fig. 4A, B). Noticed reduction in AgNP effective concentration was observed after combination with vancomycin, which ranged between one to four bi-fold reductions (Table 6). MIC values of the mixture were lower than when AgNPs were used alone for all bacterial isolates, indicating that the combination is synergistic in nature. The MIC of combination against animal bacterial isolates ranged from 0.08 to 1.25 mg/mL, whereas MIC of AgNPs alone ranged from 0.625 to 5  $\mu\text{g/mL}$ . Combination of AgNPs and vancomycin against

human bacterial isolates: the MIC of the combination ranged from 0.157 to 5  $\mu\text{g/mL}$ , whereas MIC of AgNPs alone ranged from 0.625 to 10  $\mu\text{g/mL}$ .

## Discussion

The prevalence and antibiogram profile data of bacterial isolates associated with RTI should be continuously updated due to the change of pathogen development and distribution. Scarce comparative research was conducted to evaluate the antibiotic resistance rate, biofilm formation ability, and virulence of pathogens from different origins; therefore, the RTI bacterial pathogens among humans as well as animals were characterized in this study.

The Gram-positive bacteria were the most prevalent respiratory isolates from both infected humans and animals (Table 2); *Staph. aureus* was the most frequently isolated bacterial species, which comes in accordance with previous studies.<sup>26,27</sup> Therefore, all *Staph. aureus* isolates were screened for the presence of *mecA* and *mecC* genes by conventional PCR analysis. The *mecA* gene was found to be carried by 95.0% of the isolates that display a phenotype of methicillin resistance and was detected in all multiresistant *Staph. aureus* isolates.<sup>28,29</sup> Another resistance gene called *mecC*, which is a homolog of *mecA*, has been reported to have a role in resistance process.<sup>30,31</sup>

In most reported RTI infections, the bacteria *Streptococcus* sp. and *Staphylococcus* sp. were the most recovered respiratory isolates with the variable percentage.<sup>32,33</sup> In contrast, other reports mentioned the Gram-negative species *Pseudomonas aeruginosa* and *Klebsiella pneumoniae* as the predominant strains.<sup>34–36</sup>

TABLE 4. CATEGORIZATION OF BACTERIAL ISOLATES ACCORDING TO THEIR BIOFILM FORMATION ABILITY

Isolates	Biofilm formation					
	Strong		Moderate		Non-biofilm	
	Animal ( $n=31$ ), n (%)	Human ( $n=26$ ), n (%)	Animal ( $n=21$ ), n (%)	Human ( $n=17$ ), n (%)	Animal ( $n=10$ ), n (%)	Human ( $n=7$ ), n (%)
<i>Staphylococcus aureus</i>	18 (60.00)	17 (65.35)	10 (33.33)	9 (34.61)	2 (6.66)	—
<i>Streptococcus pneumoniae</i>	4 (44.44)	5 (41.66)	3 (33.33)	3 (25.00)	2 (22.22)	4 (33.33)
<i>Listeria monocytogenes</i>	2 (50.00)	—	2 (50.00)	—	—	—
<i>Pseudomonas aeruginosa</i>	6 (46.15)	4 (33.33)	3 (23.07)	5 (41.66)	4 (30.76)	3 (25.00)
<i>Klebsiella pneumoniae</i>	1 (16.66)	—	3 (50.00)	—	2 (33.33)	—

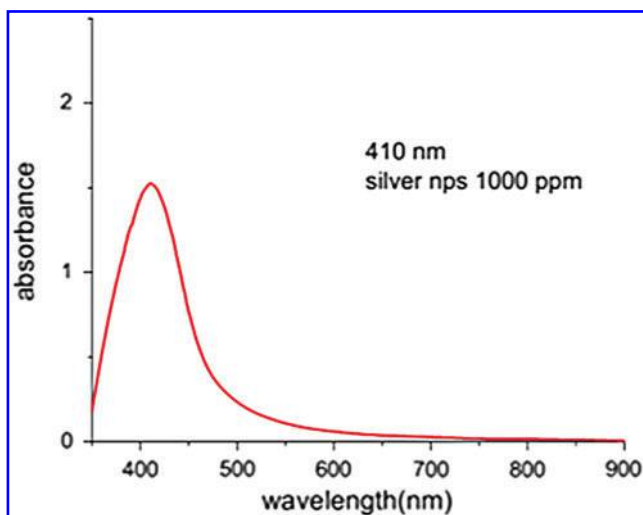


**FIG. 2.** Absorption spectrum of silver nanoparticles (AgNPs). Color images are available online.

Overall resistance pattern among isolates for commonly used antibiotics was high, but varied against one antibiotic to others (Fig. 1). In several countries, the lack of general antimicrobial resistance surveillance programs leads to inappropriate use among patients. Therefore, investigating antimicrobial resistance patterns is very critical and important, mainly in developing countries, where the antibiotic therapy should aim not only at improving the clinical outcome but also at eradicating the targeted pathogens or reducing bacterial load.<sup>37,38</sup>

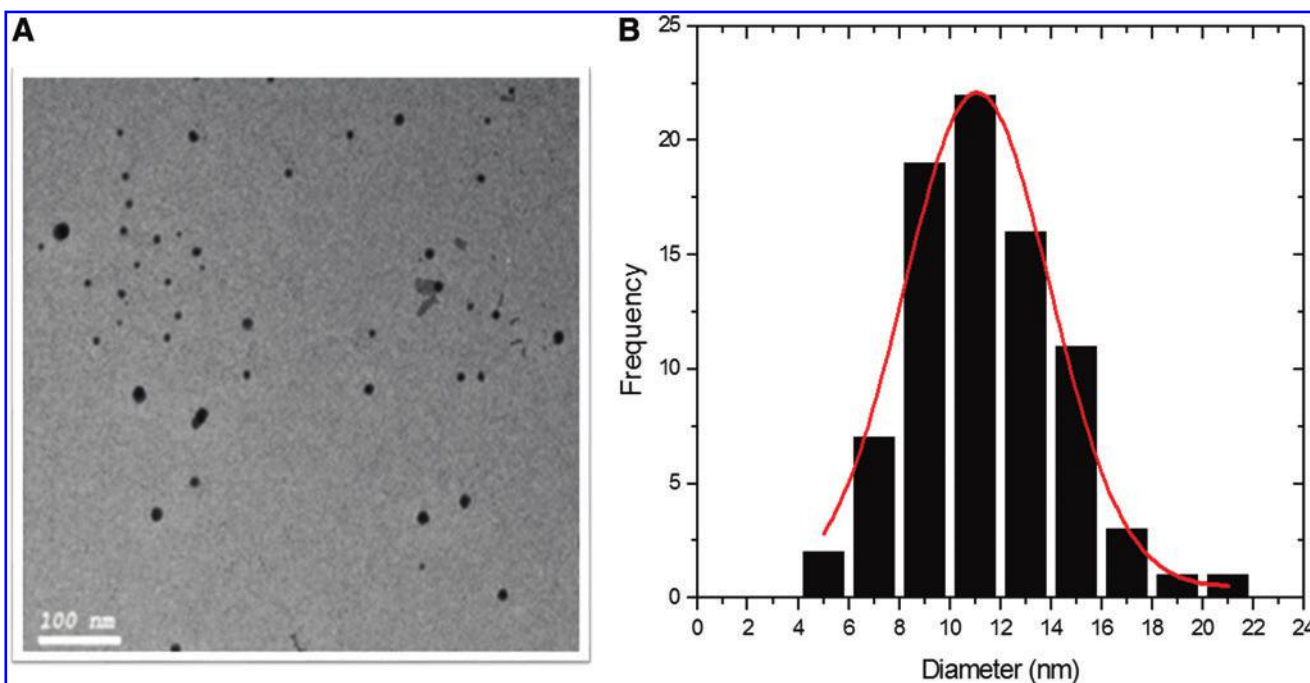
Vancomycin is the drug of choice against *Staph. aureus* with resistance rate 41.94% among animal cases. The high rate of resistance indicates that the prevalence of vanco-

mycin resistance is on the rise not only in clinical isolates but also in pathogens from animal sources. This is in line with a recent study performed in Egypt on uncooked chicken and beef meat that reported 51% vancomycin-resistant *Staph. aureus*.<sup>39</sup>

These bacterial infections are often dependent on the interplay between susceptibility of the host as well as the virulence of the associated strain. Therefore, evaluating such pathogen virulence profile helps in the evaluation of the potential outcome of infection.<sup>40</sup> In light of these, we have characterized all our different isolates for their relative biofilm-forming capacity (Table 4) and other virulence factors like gelatinase, DNAs, and hemolysin (Table 3). The *Staph. aureus* isolates were the most virulent and strongest biofilm former.

On the other hand, due to the protective nature of the biofilm extracellular matrix acting as a barrier against antimicrobial agents, biofilm-associated bacterial infections are difficult to treat, thereby causing major health care problems.<sup>41</sup> We tested both vancomycin and AgNPs for antibacterial and eradication activity of formed biofilm against a spectrum of bacterial isolates of human/animal origin representing various antibiotic resistances, biofilm compositions, and relative biofilm strengths. AgNPs were effective in inhibiting planktonic cells at low concentrations (Table 5), while regarding the biofilm eradication activity, effective values of MBEC were found to be higher than MIC values of planktonic cells, which comes in line with other studies that reported higher AgNP concentration required against biofilm-embedded bacteria, either Gram-positive or Gram-negative strains.<sup>42–44</sup>

Recently, attempts have been made to enhance the bioactivity and effectiveness of various pharmaceutical agents through the use of nanoparticle delivery methods.<sup>45</sup> Mechanisms of AgNPs that have been proposed to elucidate the killing of the bacterial cells are as follows: disruption of cellular morphology, enzyme inactivation, inhibition of



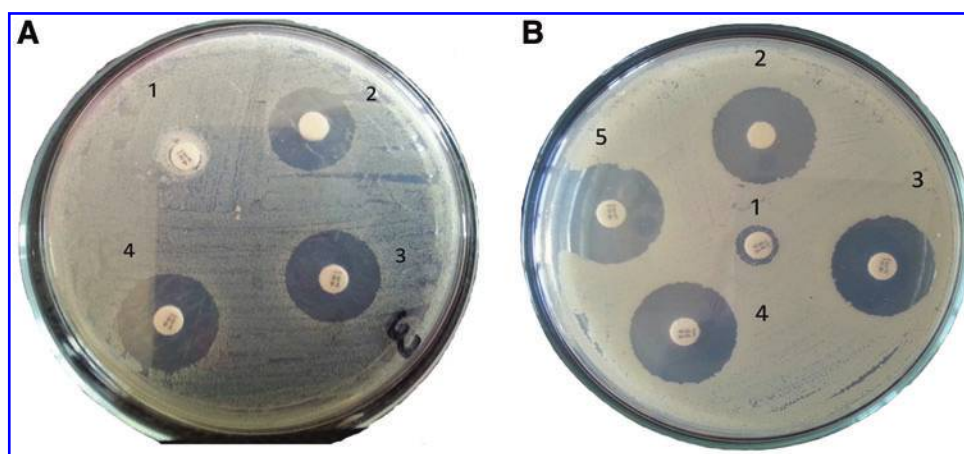
**FIG. 3.** Transmission electron microscopy micrograph of AgNPs dispersed on copper grid at 100 nm scale (A) and particle size distribution of AgNPs (B). Color images are available online.

TABLE 5. ANTIBACTERIAL EFFECT OF SILVER NANOPARTICLES AGAINST PLANKTONIC AND BIOFILM CELLS

No.	Isolates	AgNPs µg/mL			No.	Isolates	AgNPs µg/mL		
		MIC	MBC	MBEC			MIC	MBC	MBEC
1a	<i>Staphylococcus aureus</i>	2.5	2.5	2.5	57a	<i>Klebsiella pneumoniae</i>	1.25	2.5	1.25
2a	<i>Staph. aureus</i>	2.5	2.5	2.5	58a	<i>Kl. pneumoniae</i>	2.5	2.5	2.5
3a	<i>Staph. aureus</i>	2.5	5	5	59a	<i>Kl. pneumoniae</i>	2.5	5	5
4a	<i>Staph. aureus</i>	5	5	5	60a	<i>Kl. pneumoniae</i>	1.25	2.5	2.5
5a	<i>Staph. aureus</i>	1.25	2.5	2.5	61a	<i>Kl. pneumoniae</i>	5	10	—
6a	<i>Staph. aureus</i>	1.25	2.5	2.5	62a	<i>Kl. pneumoniae</i>	0.625	1.25	—
7a	<i>Staph. aureus</i>	1.25	2.5	2.5	1h	<i>Staph. aureus</i>	10	20	10
8a	<i>Staph. aureus</i>	1.25	5	5	2h	<i>Staph. aureus</i>	5	10	5
9a	<i>Staph. aureus</i>	2.5	2.5	2.5	3h	<i>Staph. aureus</i>	2.5	2.5	2.5
10a	<i>Staph. aureus</i>	2.5	2.5	2.5	4h	<i>Staph. aureus</i>	2.5	2.5	2.5
11a	<i>Staph. aureus</i>	2.5	2.5	2.5	5h	<i>Staph. aureus</i>	10	20	10
12a	<i>Staph. aureus</i>	2.5	5	5	6h	<i>Staph. aureus</i>	5	5	5
13a	<i>Staph. aureus</i>	2.5	5	5	7h	<i>Staph. aureus</i>	10	20	20
14a	<i>Staph. aureus</i>	2.5	2.5	2.5	8h	<i>Staph. aureus</i>	10	20	10
15a	<i>Staph. aureus</i>	1.25	2.5	2.5	9h	<i>Staph. aureus</i>	2.5	2.5	2.5
16a	<i>Staph. aureus</i>	2.5	5	5	10h	<i>Staph. aureus</i>	10	20	20
17a	<i>Staph. aureus</i>	1.25	2.5	2.5	11h	<i>Staph. aureus</i>	2.5	2.5	2.5
18a	<i>Staph. aureus</i>	2.5	5	5	12h	<i>Staph. aureus</i>	10	10	10
19a	<i>Staph. aureus</i>	2.5	2.5	2.5	13h	<i>Staph. aureus</i>	5	10	5
20a	<i>Staph. aureus</i>	2.5	5	5	14h	<i>Staph. aureus</i>	5	10	5
21a	<i>Staph. aureus</i>	2.5	5	5	15h	<i>Staph. aureus</i>	10	10	10
22a	<i>Staph. aureus</i>	2.5	2.5	2.5	16h	<i>Staph. aureus</i>	5	10	5
23a	<i>Staph. aureus</i>	2.5	2.5	2.5	17h	<i>Staph. aureus</i>	5	10	5
24a	<i>Staph. aureus</i>	2.5	2.5	2.5	18h	<i>Staph. aureus</i>	5	10	5
25a	<i>Staph. aureus</i>	2.5	5	2.5	19h	<i>Staph. aureus</i>	5	10	5
26a	<i>Staph. aureus</i>	2.5	2.5	2.5	20h	<i>Staph. aureus</i>	2.5	5	2.5
27a	<i>Staph. aureus</i>	2.5	2.5	2.5	21h	<i>Staph. aureus</i>	2.5	5	1.25
28a	<i>Staph. aureus</i>	1.25	2.5	—	22h	<i>Staph. aureus</i>	0.625	1.25	1.25
29a	<i>Staph. aureus</i>	1.25	2.5	—	23h	<i>Staph. aureus</i>	1.25	2.5	2.5
30a	<i>Staph. aureus</i>	1.25	2.5	2.5	24h	<i>Staph. aureus</i>	1.25	2.5	2.5
31a	<i>Streptococcus pneumoniae</i>	0.625	1.25	1.25	25h	<i>Staph. aureus</i>	0.625	1.25	1.25
32a	<i>Strep. pneumoniae</i>	2.5	5	2.5	26h	<i>Staph. aureus</i>	1.25	1.25	1.25
33a	<i>Strep. pneumoniae</i>	2.5	5	5	27h	<i>Strep. pneumoniae</i>	5	10	5
34a	<i>Strep. pneumoniae</i>	2.5	2.5	2.5	28h	<i>Strep. pneumoniae</i>	2.5	5	5
35a	<i>Strep. pneumoniae</i>	1.25	2.5	2.5	29h	<i>Strep. pneumoniae</i>	1.25	2.5	1.25
36a	<i>Strep. pneumoniae</i>	0.625	1.25	1.25	30h	<i>Strep. pneumoniae</i>	5	10	5
37a	<i>Strep. pneumoniae</i>	5	5	5	31h	<i>Strep. pneumoniae</i>	1.25	2.5	1.25
38a	<i>Strep. pneumoniae</i>	1.25	1.25	—	32h	<i>Strep. pneumoniae</i>	2.5	5	5
39a	<i>Strep. pneumoniae</i>	1.25	2.5	—	33h	<i>Strep. pneumoniae</i>	2.5	2.5	2.5
40a	<i>Listeria monocytogenes</i>	0.625	1.25	1.25	34h	<i>Strep. pneumoniae</i>	1.25	1.25	—
41a	<i>L. monocytogenes</i>	1.25	2.5	1.25	35h	<i>Strep. pneumoniae</i>	0.625	1.25	—
42a	<i>L. monocytogenes</i>	0.625	2.5	2.5	36h	<i>Strep. pneumoniae</i>	1.25	2.5	—
43a	<i>L. monocytogenes</i>	2.5	5	5	37h	<i>Strep. pneumoniae</i>	0.625	1.25	—
44a	<i>Pseudomonas aeruginosa</i>	0.625	1.25	1.25	38h	<i>Strep. pneumoniae</i>	0.625	1.25	1.25
45a	<i>Ps. aeruginosa</i>	2.5	2.5	2.5	39h	<i>Ps. aeruginosa</i>	0.625	2.5	1.25
46a	<i>Ps. aeruginosa</i>	2.5	2.5	2.5	40h	<i>Ps. aeruginosa</i>	2.5	10	5
47a	<i>Ps. aeruginosa</i>	5	5	5	41h	<i>Ps. aeruginosa</i>	0.625	1.25	1.25
48a	<i>Ps. aeruginosa</i>	0.625	1.25	1.25	42h	<i>Ps. aeruginosa</i>	5	10	5
49a	<i>Ps. aeruginosa</i>	0.625	1.25	1.25	43h	<i>Ps. aeruginosa</i>	0.625	2.5	1.25
50a	<i>Ps. aeruginosa</i>	2.5	2.5	2.5	44h	<i>Ps. aeruginosa</i>	2.5	10	5
51a	<i>Ps. aeruginosa</i>	2.5	2.5	2.5	45h	<i>Ps. aeruginosa</i>	2.5	5	2.5
52a	<i>Ps. aeruginosa</i>	0.625	1.25	1.25	46h	<i>Ps. aeruginosa</i>	1.25	2.5	2.5
53a	<i>Ps. aeruginosa</i>	1.25	1.25	—	47h	<i>Ps. aeruginosa</i>	0.625	2.5	1.25
54a	<i>Ps. aeruginosa</i>	0.625	1.25	—	48h	<i>Ps. aeruginosa</i>	0.625	1.25	—
55a	<i>Ps. aeruginosa</i>	1.25	1.25	—	49h	<i>Ps. aeruginosa</i>	2.5	5	—
56a	<i>Ps. aeruginosa</i>	0.625	1.25	—	50h	<i>Ps. aeruginosa</i>	1.25	2.5	—

AgNP, silver nanoparticle; MBC, minimum bactericidal concentration; MBEC, minimal biofilm eradication concentration; MIC, minimal inhibitory concentration.





**FIG. 4.** Preliminary screening for synergistic effect of AgNPs and vancomycin against vancomycin resistance *Staphylococcus aureus* grown in Müller Hinton agar media for 24 h at 37°C different concentration of AgNPs were added to standard vancomycin disc (30 µg). (A) *Staph. aureus* from animal origin; 1, vancomycin disc; 2, AgNP disc (0.313 µg/mL); 3, vancomycin disc plus 5 µL AgNPs (0.313 µg/mL); 4, vancomycin disc plus 5 µL AgNPs (0.625 µg/mL), with inhibition zone diameter 6.34, 17.47, 19.18, and 20.34 mm, respectively. (B) *Staph. aureus* from human origin; 1, vancomycin disc; 2, AgNP disc (2.5 µg/mL); 3, vancomycin disc plus 5 µL AgNPs (2.5 µg/mL); 4, vancomycin disc plus 5 µL AgNPs (5 µg/mL) 5, vancomycin disc plus 5 µL AgNPs (10 µg/mL), with inhibition zone diameter 7.92, 20.38, 20.75, 21.40, and 21.82 mm, respectively. Color images are available online.

DNA replication, formation of reactive oxygen species, and generation of oxidative stress,<sup>46–48</sup> in addition to the fact that AgNPs can anchor to the bacterial cell wall and consequently infiltrate it, causing physical changes in the bacterial membrane, like the membrane damage, which can lead to cellular content leakage and bacterial death.<sup>49,50</sup>

In this investigation, AgNPs/vancomycin combination had been shown to be able to eradicate established biofilm of different bacterial species, resulting in a reduction of vancomycin effective dose ranging from onefold to fourfold reduction

**TABLE 6. BIFOLD REDUCTION OF SILVER NANOPARTICLES AFTER COMBINATION ON AGNPs WITH 1/4 MINIMAL INHIBITORY CONCENTRATION OF VANCOMYCIN**

Isolates	Bifold reduction of AgNPs			
	1	2	3	4
	No. of isolates (%)			
<i>Staphylococcus aureus</i>				
Animal (30)	5 (16.66)	15 (50)	9 (30)	1 (3.33)
Human (26)	1 (3.85)	9 (34.62)	13 (50)	3 (11.5)
<i>Streptococcus pneumoniae</i>				
Animal (9)	3 (33.33)	5 (55.56)	1 (11.11)	—
Human (12)	—	11 (91.66)	1 (8.33)	—
<i>Listeria monocytogenes</i>				
Animal (4)	2 (50)	2 (50)	—	—
Human (0)	—	—	—	—
<i>Pseudomonas aeruginosa</i>				
Animal (13)	—	4 (30.77)	9 (69.23)	—
Human (12)	5 (41.66)	7 (58.33)	—	—
<i>Klebsiella pneumonia</i>				
Animal (6)	—	—	4 (66.66)	2 (33.33)
Human (0)	—	—	—	—

(Table 6). Despite the effective dose reduction of vancomycin upon all *Staph. aureus* strains in our study, from both origins when combined with AgNPs, opposite reports were found in the literature, which agreed<sup>51,52</sup> and deny this combination activity of AgNPs/vancomycin on *Staph. aureus*.<sup>53</sup>

On the other hand, the combination effect was remarkable on the tested Gram-negative pathogens *Ps. aeruginosa* and *Kl. pneumoniae*, which comes in line with recent reports.<sup>54,55</sup> This combination effect can be explained by the high surface to volume ratio of the AgNPs as well as the increase in the bacterial cell membrane permeability damage due to the hydrophobic nature of AgNPs, leading to the transport and entrance of antimicrobial agent inside the bacterial cell.<sup>46,56</sup> Overall, those dual treatments were more effective than either treatment alone, which also comes in agreement with other reports<sup>57–59</sup>; therefore, the utilization of nanoparticles in combination with antibiotic is highly regarded.<sup>60,61</sup>

In conclusion, the possible zoonotic transmission of antibiotic resistance and biofilm growing pathogen is an alarm to public health. Our study demonstrates the prevalence of *Staph. aureus* among RTI pathogens in animal and human. The prevalence of antibiotic resistance and high ability to produce virulence factors and biofilm were also reported. Strong antibacterial and biofilm eradication activity of AgNPs alone and in combination with reduced concentration of both agents (1/4 MIC of vancomycin + serial dilution of AgNPs) were concluded in our study. In addition, the potential use of effective antimicrobial dose of AgNPs against MDR pathogens mixed with futile antibiotic is suggested as a possible final line of treatment.

#### Authors' Contributions

All authors were involved in the conception of the research idea, methodology design, in particular M.S.M.M., Z.K., and S.I.A. Both H.M.M. and M.S.M.M. carried out the laboratory work. H.H.M. and S.I.A. collected the bacterial



strains from both sources. H.M.M., S.H.M., and M.S.M.M. interpreted the results and prepared the article for publication. Z.K., M.S.M.M., and S.H.M. reviewed the article. All authors read and approved the final article.

#### Disclosure Statement

No competing financial interests exist.

#### Funding Information

No funding was received.

#### References

1. Matthews, L., R.K. Kanwar, S. Zhou, V. Punj, and J.R. Kanwar. 2010. Applications of nanomedicine in antibacterial medical therapeutics and diagnostics. *Open Trop. Med. J.* 3: 1–9.
2. Mohamed, M.S.M., A.A. Abdallah, M.H. Mahran, and M. Shalaby. 2018. Potential alternative treatment of ocular bacterial infections by oil derived from *Syzygium aromaticum* flower (Clove). *Curr. Eye Res.* 43:873–881.
3. Ventola, C.L. 2015. The antibiotic resistance crisis part 1: causes and threats. *Pharm. Ther.* 40:277–283.
4. Cheesman, M.J., A. Ilanko, B. Blonk, and I.E. Cock. 2017. Developing new antimicrobial therapies: are synergistic combinations of plant extracts/compounds with conventional antibiotics the solution? *Pharmacogn. Rev.* 11:57–72.
5. Rodrigo-Troyano, A., and O. Sibila. 2017. The respiratory threat posed by multidrug resistant Gram-negative bacteria. *Asian Pacific Soc. Respirol.* 22:1288–1299.
6. De Benedetto, F., and G. Sevieri. 2013. Prevention of respiratory tract infections with bacterial lysate OM-85 bronchomunal in children and adults: a state of the art. *Multidiscip. Respir. Med.* 8:33.
7. Cheng, G., M. Dai, S. Ahmed, H. Hao, and X. Wang. 2016. Antimicrobial drugs in fighting against antimicrobial resistance. *Front. Microbiol.* 7:470.
8. Morris, D.P. 2007. Bacterial biofilm in upper respiratory tract infections. *Curr. Infect. Dis. Rep.* 9:186–192.
9. Corno, S., and M. Garotta. 2010. Biofilms and infections of the upper respiratory tract. *Eur. Rev. Med. Pharmacol. Sci.* 14:683–690.
10. Pang, X., Y. Yang, and H. Yuk. 2017. Biofilm formation and disinfectant resistance of *Salmonella* sp. in mono- and dual-species with *Pseudomonas aeruginosa*. *J. Appl. Microbiol.* 123:651–660.
11. Chintamani, R.B., K.S. Salunkhe, and M.J. Chavan. 2018. Emerging use of green synthesis silver nanoparticle: an update review. *Int. J. Pharm. Sci. Res.* 9:4029–4055.
12. Tiwari, V., M.K. Khokar, M. Tiwari, S. Barala, and M. Kumar. 2014. Anti-bacterial activity of polyvinyl pyrrolidone capped silver nanoparticles on the carbapenem resistant strain of *Acinetobacter baumannii*. *J. Nanomed. Nanotechnol.* 5: 1000246.
13. Kamel, Z., M. Saleh, and N. El Namoury. 2016. Biosynthesis, characterization, and antimicrobial activity of silver nanoparticles from *Actinomyces*. *Res. J. Pharm. Biol. Chem. Sci.* 7:119–127.
14. Burdusel, A.-C., O. Gherasim, A.M. Grumezescu, M. Laurentiu, A. Ficai, and E. Andronescu. 2018. Biomedical applications of silver nanoparticles: an up-to-date overview. *Nanomaterials* 8:681.
15. Bergey, D.H. 2009. *Bergey's Manual of Systematic Bacteriology*. Firmicutes, Vol. 3. Springer-Verlag, New York, pp. 1–1476.
16. Clinical and Laboratory Standards Institute. 2012. *Methods for Dilution Antimicrobial Susceptibility Tests for Bacteria That Grow Aerobically*; CLSI Document M07-A9, 9th ed. CLSI, Wayne, PA.
17. Clinical and Laboratory Standards Institute. 2012. *Performance Standards for Antimicrobial Susceptibility Testing; Twenty-Second Informational Supplement*. Clinical and Laboratory Standards Institute, Wayne, PA.
18. Stegger, M., P.S. Andersen, A. Kearns, B. Pichon, M.A. Holmes, G. Edwards, F. Laurent, C. Teale, R. Skov, and A.R. Larsen. 2012. Rapid detection, differentiation and typing of methicillin-resistant *Staphylococcus aureus* harbouring either *mecA* or the new *mecA* homologue *mecALGA251*. *Clin. Microbiol. Infect.* 18:395–400.
19. Fazlul, M., A. Najnin, Y. Farzana, M. Rashid, S. Deepthi, C. Srikumar, S.S. Rashid, and M. Nazmul. 2018. Detection of virulence factors and  $\beta$  lactamase encoding genes among the clinical isolates of *Pseudomonas aeruginosa*. *J. Int. Pharm. Res.* 45:190–202.
20. Mohamed, S.H., D. Salem, M. Azmy, and N.S. Fam. 2018. Antibacterial and antibiofilm activity of cinnamaldehyde against carbapenem-resistant *Acinetobacter baumannii* in Egypt: *in vitro* study. *J. Appl. Pharm. Sci.* 8:151–156.
21. Sahoo, P.K., S.S.K. Kamal, T.J. Kumar, B. Sreedhar, A.K. Singh, and S.K. Srivastava. 2009. Synthesis of silver nanoparticles using facile wet chemical route. *Def. Sci. J.* 59: 447–455.
22. Mohamed, S.H., M.S.M. Mohamed, M.S. Khalil, W.S. Mohamed, and M.I. Mabrouk. 2018. Antibiofilm activity of papain enzyme against pathogenic *Klebsiella pneumoniae*. *J. Appl. Pharm. Sci.* 8:163–168.
23. Singh, P., Y.J. Kim, H. Singh, C. Wang, K.H. Hwang, M.E. Farh, and D.C. Yang. 2015. Biosynthesis, characterization, and antimicrobial applications of silver nanoparticles. *Int. J. Nanomedicine* 10:2567–2577.
24. Ebrahimi, A., H. Azarban, S. Habibian, M. Mahzunieh, and S. Lotfalian. 2017. Evaluation of anti-biofilm and antibiotic synergistic activities of silver nanoparticles against some common bacterial pathogens. *Int. J. Basic Sci. Med.* 2:128–132.
25. Magiorakos A.P., A. Srinivasan, R.B. Carey, Y. Carmeli, M.E. Falagas, C.G. Giske, and D.L. Monnet. 2012. Multidrug-resistant, extensively drug-resistant and pandrug-resistant bacteria: an international expert proposal for interim standard definitions for acquired resistance. *Clin. Microbiol. Infect.* 18: 268–281.
26. Eldeeb, A.H., and E.M. Khashan. 2002. Microbiological study on respiratory tract infections in libya. *Egypt J. Hosp. Med.* 24:442–459.
27. Mandal, A.K., P. Pratip, and K. Kundu. 2018. Antibiotic susceptibility pattern of bacterial strains isolated from children with upper respiratory tract infection. *J. Dent. Med. Sci.* 17:1–6.
28. Wielders, C.L.C., A.C. Fluit, S. Brisse, J. Verhoef, and F.J. Schmitz. 2002. *mecA* gene is widely disseminated in *Staphylococcus aureus* population. *J. Clin. Microbiol.* 40: 3970–3975.
29. Jakab, E., M. Colcieru, R.I. Jakab, E.E. Gabri, C.H. Lázár, E. Török, B. Kremmer, T.J. Mészáros, Á. Katona, E. Fazakas, L. Coldea, and O. Popescu. 2019. Screening of *mecI* gene in *Staphylococcus* strains isolated in

- transylvania region of Romania. *Microb. Drug Resist.* 25:639–643.
30. Deplano, A., S. Vandendriessche, C. Nonhoff, and O. Denis. 2014. Genetic diversity among methicillin-resistant *Staphylococcus aureus* isolates carrying the *mecC* gene in Belgium. *J. Antimicrob. Chemother.* 69:1457–1460.
  31. Cikmana, A., M. Aydina, B. Gulhana, F. Karakeçili, M.G. Kurtoglud, S. Yuksekkaya, M. Parlakf, B.S. Gultepeg, A.C. Cicek, F.B. Bilman, I.H. Ciftci, M. Kara, S. Atmaca, and T. Ozekinci. 2019. Absence of the *mecC* gene in methicillin-resistant *Staphylococcus aureus* isolated from various clinical samples: the first multi-centered study in Turkey. *J. Infect. Public Health* 12:528–533.
  32. Praveen, S., A. Prema, and A. Routray. 2013. Prevalence and antibiotic susceptibility pattern of bacterial agents causing respiratory tract infection in Children. *JPR Bio-MedRx Int. J.* 1:596–598.
  33. Atia, A., A. Abired, A. Ammar, N. Elyounsi, and A. Ashour. 2018. Prevalence and types of bacterial infections of the upper respiratory tract at a tertiary care hospital in the city of Tripoli. *Libyan Int. Med. Univ. J.* 3:54–58.
  34. Sarmah, N., A. Sarmah, and D.K. Das. 2016. A study on the microbiological profile of respiratory tract infection (RTI) in patients attending gauhati medical college & hospital. *Ann. Int. Med. Dent. Res.* 2:11–15.
  35. Vijay, S., and G. Dalela. 2016. Prevalence of LRTI in patients presenting with productive cough and their antibiotic resistance pattern. *J. Clin. Diagnostic Res.* 10: DC09–DC12.
  36. AL-Fatlawi, A.A.A. 2019. Isolation and antibiotic resistance of *P. aeruginosa* isolated from upper respiratory tract infection in Najaf governorate. *Al-Kufa Univ. J. Biol.* 7: 255–264.
  37. Blasi, F., E. Concia, B. Prato, M. Giusti, B. Polistena, A. Rossi, S. Stefani, A. Novelli; and on behalf of the MASTER working group. 2017. The most appropriate therapeutic strategy for acute lower respiratory tract infections: a Delphi- based approach. *J. Chemother.* 29: 274–186.
  38. Azimi, T., S. Maham, F. Fallah, L. Azimi, and Z. Gholinejad. 2019. Evaluating the antimicrobial resistance patterns among major bacterial pathogens isolated from clinical specimens taken from patients in Mofid Children's Hospital, Tehran, Iran: 2013–2018. *Infect. Drug Resist.* 12: 2089–2102.
  39. Osman, K.M., A.M. Amer, J.M. Badr, A.S.A. Saad. 2015. Prevalence and antimicrobial resistance profile of staphylococcus species in chicken and beef raw meat in Egypt. *Foodborne Pathog. Dis.* 12:406–413.
  40. Stephenson, S., and P. Brown. 2016. Distribution of virulence determinants among antimicrobial-resistant and antimicrobial-susceptible *Escherichia coli* implicated in urinary tract infections. *Indian J. Med. Microbiol.* 34:448–456.
  41. Graf, A.C., A. Leonard, M. Schäuble, L.M. Rieckmann, J. Hoyer, S. Maaß, M. Lalk, D. Becher, J. Pané-farré, and K. Riedel. 2019. Virulence factors produced by *Staphylococcus aureus* biofilms have a moonlighting function contributing to biofilm integrity. *Mol. Cell. Proteomics* 18: 1036–1053.
  42. Goswami, S.R., T. Sahareen, M. Singh, and S. Kumar. 2015. Role of biogenic silver nanoparticles in disruption of cell – cell adhesion in *Staphylococcus aureus* and *Escherichia coli* biofilm. *J. Ind. Eng. Chem.* 26: 73–80.
  43. Sharma, B.K., A. Saha, L. Rahaman, S. Bhattacharjee, and P. Tribedi. 2015. Silver inhibits the biofilm formation of *Pseudomonas aeruginosa*. *Adv. Microbiol.* 6: 677–685.
  44. Barapatre, A., K.R. Aadil, and H. Jha. 2016. Synergistic antibacterial and antibiofilm activity of silver nanoparticles biosynthesized by lignin-degrading fungus. *Bioresour. Bio-process.* 3:1–13.
  45. Patra, J.K., G. Das, L.F. Fraceto, E.V.R. Campos, M. del P. Rodriguez-Torres, L.S. Acosta-Torres, L.A. Diaz-Torres, R. Grillo, M.K. Swamy, S. Sharma, S. Habtemariam, and H.S. Shin. 2018. Nano based drug delivery systems: recent developments and future prospects. *J. Nanobiotechnology* 16:71.
  46. Gomaa, E.Z. 2017. Silver nanoparticles as an antimicrobial agent: a case study on *Staphylococcus aureus* and *Escherichia coli* as models for Gram-positive and Gram-negative bacteria. *J. Gen. Appl. Microbiol.* 63:36–43.
  47. Rongtao, Z., L. Min, L. Yang, S. Mingxuan, K. Wen, W. Lihua, S. Shiping, F. Chunhai, J. Leili, Q. Shaofu, S. Yansong, S. Hongbin, and H. Rongzhang. 2017. Stable nanocomposite based on PEGylated and silver nanoparticles loaded graphene oxide for long-term antibacterial activity. *ACS Appl. Mater. Interfaces.* 9:15328–15341.
  48. Pompilio, A., C. Geminiani, D. Bosco, R. Rana, A. Aceto, T. Bucciarelli, L. Scotti, and D. Bonaventura. 2018. Electrochemically synthesized silver nanoparticles are active against planktonic and biofilm cells of *Pseudomonas aeruginosa* and other cystic fibrosis-associated bacterial pathogens. *Front. Microbiol.* 9:1349.
  49. Khalandi, B., N. Asadi, M. Milani, S. Davaran, A.J.N. Abadi, E. Abasi, and A. Akbarzadeh. 2017. A review on potential role of silver nanoparticles and possible mechanisms of their actions on Bacteria. *Drug Res.* 67:70–76.
  50. Seong, M., and D.G. Lee. 2017. Silver nanoparticles against *Salmonella enterica* serotype typhimurium: role of inner membrane dysfunction. *Curr. Microbiol.* 74: 661–670.
  51. Kaur, A., and R. Kumar. 2019. Enhanced bactericidal efficacy of polymer stabilized silver nanoparticles in conjugation with different classes of antibiotics. *R. Soc. Chem.* 9:1095–1105.
  52. Labruère, R., A. Sona, and E. Turos. 2019. Anti-methicillin-resistant *Staphylococcus aureus* nanoantibiotics. *Front. Pharmacol.* 10:1121.
  53. Akram, F.E., T. El-Tayeb, K.A. Aisha, and M. El-Azizi. 2016. A combination of silver nanoparticles and visible blue light enhances the antibacterial efficacy of ineffective antibiotics against methicillin-resistant *Staphylococcus aureus* (MRSA). *Ann. Clin. Microbiol. Antimicrob.* 15:48.
  54. Naqvi, S.Z.H., U. Kiran, M.I. Ali, A. Jamal, A. Hameed, S. Ahmed, and N. Ali. 2013. Combined efficacy of biologically synthesized silver nanoparticles and different antibiotics against multidrug-resistant bacteria. *Int. J. Nanomedicine.* 8:3187–3195.
  55. Nayak, B., and K. Anitha. 2014. Amplified antibiotic potency of two different drugs combined with biosynthesized AgNPs from *Aspergillus sydowii* isolated from sand dunes. *Int. J. Pharm. Tech. Res.* 6:1751–1755.
  56. Esmaeillou, M., G. Zarrini, M.A. Rezaee, J.S. Mojarrad, and A. Bahadori. 2017. Vancomycin capped with silver

- nanoparticles as an antibacterial agent against multi-drug resistance bacteria. *Adv. Pharm. Bull.* 7:479–483.
57. Fayaz, A.M., K. Balaji, M. Girilal, R. Yadav, P.T. Kalaichelvan, and R. Venketesan. 2010. Biogenic synthesis of silver nanoparticles and their synergistic effect with antibiotics: a study against gram-positive and gram-negative bacteria. *Nanomed. Nanotechnol. Biol. Med.* 6: 103–109.
  58. McShan, D., Y. Zhang, H. Deng, P.C. Ray, and H. Yu. 2015. Synergistic antibacterial effect of silver nanoparticles combined with ineffective antibiotics on drug resistant *Salmonella typhimurium* DT104. *J. Environ. Sci. Heal.* 33: 369–384.
  59. Hair, B., M. Conley, T. Wienclaw, M. Conley, M. Heaton, and B. Berges. 2018. Synergistic activity of silver nanoparticles and vancomycin against a spectrum of *Staphylococcus aureus* biofilm types. *J. Bacteriol. Mycol.* 5:1089.
  60. Cho, Y., Y. Mizuta, J. Akagi, T. Toyoda, M. Sone, and K. Ogawa. 2018. Size-dependent acute toxicity of silver nanoparticles in mice. *J. Toxicol. Pathol.* 2018; 31:73–80.
  61. Mao, B., Z. Chen, Y. Wang, and S. Yan. 2018. Silver nanoparticles have lethal and sublethal adverse effects on development and longevity by inducing ROS-mediated stress responses. *Sci. Rep.* 8:2445.

Address correspondence to:  
*Mahmoud S.M. Mohamed, PhD*  
*Department of Botany and Microbiology*  
*Faculty of Science*  
*Cairo University*  
*Giza 12613*  
*Egypt*

*E-mail:* msaleh@sci.cu.edu.eg

**This article has been cited by:**

1. Hamada AbdElgawad, Yasser M. Hassan, Modhi O. Alotaibi, Afrah E. Mohammed, Ahmed M. Saleh. 2020. C3 and C4 plant systems respond differently to the concurrent challenges of mercuric oxide nanoparticles and future climate CO2. *Science of The Total Environment* **749**, 142356. [[Crossref](#)]
2. Sara H. Mohamed, Maram M.S. Elshahed, Yasmine M. Saied, Mahmoud S.M. Mohamed, Gamal H. Osman. 2020. Detection of Heavy Metal Tolerance among different MLSB Resistance Phenotypes of Methicillin-Resistant S. aureus (MRSA). *Journal of Pure and Applied Microbiology* **14**:3, 1905-1916. [[Crossref](#)]